(2)

SEC

AD-A214 762	IMENTATION PAGE	Form Approved OMB No. 0704-0188
1a.		1b RESTRICTIVE MARKINGS
2a.		3. DISTRIBUTION/AVAILABILITY OF REPORT Approved for public release; distribution unlimited.
2b. DECLASSIFICATION/DOWNGRADING SCHEDULE	NOV 30 1989	
4. PERFORMING ORGANIZATION REPORT NUMBER(S)		5. MONITORING ORGANIZATION REPORT NUMBER(S) AFOSR-TR- 89-1450
6a. NAME OF PERFORMING ORGANIZATION University of California Department of Physics,	6b. OFFICE SYMBOL (If applicable)	7a. NAME OF MONITORING ORGANIZATION AFOSR
6c. ADDRESS (City, State, and ZIP Code) 405 Hilgard Ave Los Angeles, California 90024		7b. ADDRESS (City, State, and ZIP Code) BLDG 410 BAFB DC 20332-6448
8a. NAME OF FUNDING/SPONSORING ORGANIZATION AFOSR	8b. OFFICE SYMBOL (If applicable)	9 PROCUREMENT INSTRUMENT IDENTIFICATION NUMBER F49620-76-C-0011
8c. ADDRESS (City, State, and ZIP Code) BLDG 410 BAFB DC 20332-6448		10 SOURCE OF FUNDING NUMBERS

PROGRAM ELEMENT NO.	PROJECT NO.	TASK NO	WORK UNIT ACCESSION NO.
61102F	2301	A7	

11. TITLE (Include Security Classification)
SIMULATION OF IONOSPHERIC EM-PLASMA INTERACTION IN A LARGE LABORATORY DEVICE

12. PERSONAL AUTHOR(S)
A.Y. Wong and Dennis Eggleston

13a. TYPE OF REPORT	13b. TIME COVERED	14. DATE OF REPORT (Year, Month, Day)	15. PAGE COUNT
Final	FROM ____ TO ____	November 21, 1979	18

16. SUPPLEMENTARY NOTATION

17. COSATI CODES			18. SUBJECT TERMS (Continue on reverse if necessary and identify by block number)
FIELD	GROUP	SUB-GROUP	

19. ABSTRACT (Continue on reverse if necessary and identify by block number)

The evolution of cavitons in two-dimensions is studied by measuring the space and time development of the caviton electric field. For low power drivers the cabiton is found to have an Airy function type shape which is stable in time. When a high power driving electric field is used, however, the caviton shape becomes chaotic due to nonlinear modification of the density profile. In two-dimensions, the cabiton electric field is seen to develop a component in the direction perpendicular to the driving field; the initial azimuthal symmetry of the caviton is also destroyed.

68

20 DISTRIBUTION/AVAILABILITY OF ABSTRACT	21 ABSTRACT SECURITY CLASSIFICATION	
☒ UNCLASSIFIED/UNLIMITED ☐ SAME AS RPT ☐ DTIC USERS	unclassified	
22a NAME OF RESPONSIBLE INDIVIDUAL	22b TELEPHONE (Include Area Code) 767-4904	22c OFFICE SYMBOL NP

DD Form 1473, JUN 86 Previous editions are obsolete. SECURITY CLASSIFICATION OF THIS PAGE

AFOSR-TR- 89-1450

FINAL SCIENTIFIC REPORT

for

AFOSR Contract F49620-76-C-0011

SIMULATION OF IONOSPHERIC EM-PLASMA

INTERACTION IN A LARGE LABORATORY DEVICE

October 1, 1978 - September 30, 1979

A. Y. Wong, Principal Investigator
University of California
Los Angeles, California 90024

INTRODUCTION

When a P-polarized EM wave is obliquely incident on a plasma density gradient, linear conversion to ES waves can occur in the vicinity of the point where $\omega = \omega_{pe}$. More precisely, the EM wave is reflected at the cutoff point where $\omega_{pe} = \omega \cos\theta$, where θ is the angle between $\underline{k}_{EM}$ and $\underline{\nabla} n_0$; beyond this point the electric field is evanescent. This evanescent field, directed along $\underline{\nabla} n_0$, can drive an electrostatic resonance at the point where $\omega = \omega_{pe}$. The evanescent driver is strongly enhanced (typically 100 - 1000x) in this region and the ponderomotive force of the localized electric field can form density cavities. This field-cavity entity is what we call a caviton[1].

In order to study the caviton in detail it is not necessary to use the linear conversion of EM to ES waves; one can instead use an oscillating longitudinal driver to simulate the evanescent field. The advantage of using this technique comes with the reduction of typical scale lengths. The study of EM propagation and reflection requires (in order to avoid finite geometry effects) a chamber large compared to the EM wavelength, whereas the caviton requires a chamber large compared to the wavelength of an electron plasma wave. It is easy to show that $\lambda_{EM}/\lambda_{ES} = c/\sqrt{3T_e/m} \simeq 400$ for $T_e = 1$ eV. Thus the detailed study of the caviton can be done in a small chamber (which is advantageous in terms of construction cost and maintenance as well as diagnosis) while the "big picture" including EM effects can be studied in a large device.

EXPERIMENTAL DEVICE

This year our experimental work has focussed on the study of cavitons in two dimensions. The cylindrically symmetric device shown in Fig. 1 was constructed for this study. It has several advantages over the 1-D capacitor plate driven system used formerly to study cavitons in one dimension. A pulsed 1 kW, HF (20 MHz) oscillator is connected to a long, cylindrically symmetric

antennae to produce the plasma. The density gradient in the experimental region is in the radial direction and the coaxial line formed by the central rod and the chamber wall can be driven in the TEM mode (f = 285 MHz) to give a purely radial driving electric field; this is in contrast to the 1-D capacitor plate experiment where fringing driver fields in the direction perpendicular to the density gradient are unavoidable. The cylindrical geometry allows one of the directions perpendicular to the density gradient to close on itself, thus avoiding boundary effects. Finally, the newly developed two-dimensional scanning diagnostic electron beam allows for a complete study of the caviton's space and time evolution. The electron beam is an unperturbing diagnostic with a time resolution of 0.2 μs and a spatial resolution of approximately one millimeter. We have found it to be the best and perhaps the only reliable diagnostic for measuring RF electric fields in a plasma. The beam, which is capable of moving both radially and azimuthally, traverses the chamber axially and is modulated by the radially localized caviton electric field. It then strikes a phosphor-coated window and produces an image which depends on the amplitude and direction of the caviton field. After measuring the axially dependence of the caviton one can unfold this image data and determine the field values.

A word about the importance of measuring the electric field is in order. One might suppose that the shape and size of the caviton electric field could be inferred from the associated density cavities. While this may be valid in a general sense, it has two crucial limitations. First of all, the density cavities form on a much slower time scale than the caviton electric fields; this is simply due to the fact that ion inertia is so much greater than that of the electrons. For the same reason, density cavities will remain long after

the electric field is gone. Secondly, in order to avoid spurious probe measurements one must measure the plasma density profile only after the driving VHF burst has ended (typically at least 1 μs after). Thus one is reduced to looking at density profiles that may be significantly changed from those existing 1-2 μs earlier. Thus although one might infer things about the electric field from the density cavities in a static situation, one cannot use such a method for a detailed analysis of a quickly changing phenomena like the caviton.

The device is fitted with two sets of magnetic field coils. The first set (not shown) consists of large, perpendicularly oriented Helmholtz coils to cancel out the Earth's magnetic field; this is necessary in order for the e-beam to follow a straight trajectory. The second set produces an axial magnetic field uniform to within 5% over the experimental area. These coils will allow us to study upper-hybrid cavitons.

EXPERIMENTAL RESULTS

Figure 2 shows a box diagram of the basic setup for our experiments. An Argon plasma is produced by a pulsed HF discharge; at a selected time in the discharge afterglow a short (1 - 10 μs) VHF pulse ($f = 285$ MHz, $P \leq 100$ watts) is applied to the center electrode of the chamber to act as the driver for the cavitons. At a selected time within the VHF pulse a short (≤ 1 μs) pulse is applied to the electron gun deflection plates. The image produced on the phosphorous screens by the electrons gives the amplitude and direction of the caviton electric field at the selected time and the selected radial and azimuthal position. In addition time resolved density profiles are obtained with a movable Langmuir probe and boxcar averager.

Figure 3 shows the maximum magnitude of the caviton electric field when the experiment is performed at various times in the discharge afterglow. For early

times in the afterglow the electron temperature is high and transit time damping by tail electrons effectively limits the electric field enhancement.[3] As the electron temperature falls the population of tail electrons decreases, thus reducing the damping and increasing sharply the electric field enhancement. The fall of the electric field at still later times is not well understood at present but may be due to changes in the plasma density scale length. All the following experiments were performed at an afterglow time of 50 μs.

Figure 4 shows a radial scan of the electric field magnitude and its correlation with associated density cavities. A 1 μs VHF pulse is used; the top trace is obtained with the diagnostic electron beam during the VHF pulse. The bottom trace is the radial density profile obtained with a Langmuir probe sampled 1 μs after the end of the VHF pulse. The dotted line shows the shape of the profile before the VHF burst is applied. Since there are two points on this profile where $\omega = \omega_{pe}$, two cavitons are formed and the coalesce of the two formed the large cavity extending from R = 3 - 7 cm. The electric field due to the caviton on the left is beyond the range of the electron beam and thus is not shown.

The time evolution of the caviton fields is shown in Figure 5. A low-power, 7 μs long VHF burst is applied and the electron beam is used to measure the field applitude at four times within the burst. The initial radial profile is seen to have the shape of the well known Airy function. The Airy function is the solution to the problem of driving a linear density gradient with a uniform pump -- the so-called capacitor plate problem.[1] This is the first observation of such an electric field amplitude profile; generally the smaller peaks have not been observed.

As we look at the time evolution of this profile we notice some small changes.

The entire profile is moving to the left; this is due to the continuing decay of the plasma density. Other changes are also evident - changes in amplitude, width, and spacing of the various peaks. Since the profile is continually being modified by the ponderomotive force of the electric field peaks it is not surprising that the profiles are not exactly the same as that for a linear density gradient. The point here is that for low-power excitation the profiles remain qualitatively the same; a large main peak followed by two or three smaller peaks occuring further down the density gradient. This is in marked contrast to the field profile behavior for high-power VHF bursts. Figure 6 shows the profile evolution for a 100 watt; 9 μs burst. Although the profile is initially Airy-like, it quickly becomes irregular as the density profile is strongly modified. The associated density profile modification is shown in Figure 7, where the density is measured 1 μs after the end of the VHF burst. Through the formation of multiple cavities, the initially smooth and linear density profile becomes pitted and chaotic.

Up to this point our data has only shown the one dimensional behavior of the caviton, all the data having been taken at one azimuthal position ($\theta = 90°$). Figures 8 and 9 show the field amplitude profiles for various azimuthal positions near $\theta = 90°$ for the case of a high power driver. Figure 8 is taken at $t = 1$ μs within the VHF burst. It shows that the field profiles are roughly Airy-like and that no striking azimuthal dependence exists; from this we infer that the driver and density profile initially exhibit no azimuthal dependence. At later times ($t = 7$ μs) with the VHF burst, we observe two things (see Figure 9). First of all, the radial profiles have become chaotic as in Figure 6. The solid lines show that in addition to becoming radially chaotic that some azimuthal variation has developed. The second effect concerns the direction of the electric field. Up to this point all the measured electric fields have been purely radial; i.e.

in the same direction as the driver, as one would expect. Now, however, we observe the development of an electric field component in the azimuthal direction, as shown by the dotted line. This azimuthal field is comparable in amplitude to the radial field and is localized radially and azimuthally.

The observation of this azimuthally-directed field was quite unexpected and points out the usefulness of the electron beam diagnostic which can measure fields in both the radial and azimuthal directions. This phenomena has not been observed previously and our data at the time of this report does not allow us to make any conclusions about its source although one might infer that it is somehow associated with the extensive density profile modification. We can, at least, say that the data indicates the usefulness of such a two-dimensional study and may have important application to critical layer phenomena in both ionospheric and laser-pellet physics.

Personnel Associated with the Research Effort:

Full and part time students:	Dennis Eggleston Chris Darrow
Support Personnel:	G. Neff P. Wells
Principal Investigator:	Alfred Y. Wong

REFERENCES

1. A. Y. Wong, "Electromagnetic Wave Interactions with Inhomogeneous Plasmas" in Laser Interaction and Related Plasma Phenomena, Vol. 4B, pp. 733-840, Plenum Publishing Corp., 1977.

2. H. C. Kim, R. L. Stenzel and A. Y. Wong, Phys. Rev. Lett. 33, 886, (1974).

3. A. Y. Wong, P. Leung, and D. L. Eggleston, Phys. Rev. Lett. 39, 1407 (1977).

4. G. J. Morales and Y. C. Lee, Phys. Rev. Lett. 33, 1016 (1974).

Following is the title and abstract of our work performed under ARCSR Contract AF-F49620-76-C-0011 which was presented at the American Physical Society Meeting, Boston, Massachusetts, November 12 - 16, 1979.

255 Resonantly Enhanced Electric Fields in a Two-Dimensional Caviton.* D. L. Eggleston, C. B. Darrow, A. Y. Wong, UCLA.--Our earlier[1] experimental investigations of RF-plasma interactions in a plasma-filled coaxial line have been extended to include a detailed study of resonantly enhanced electric fields for the unmagnetized and magnetized ($\omega_{pe}/\omega_{ce} \geq 3$) case as well as the case of an azimuthally non-uniform driver $\underline{E}_0 = \underline{E}_0(r,\theta)$. A non-perturbing 2-D scanning diagnostic electron beam is used to measure the amplitude, direction, and spatial dependence of the enhanced fields near the resonant region ($\omega \approx \omega_{pe}, \omega_{uh}$). The time evolution of these fields is studied using a sampled electron beam technique. Transit time damping of the resonant electric fields by electrons is identified and controlled[2]. The effect of an azimuthally non-uniform driver is studied by splitting the coaxial center conductor and driving the two halves out of phase.

1. D. L. Eggleston and A. Y. Wong, Bull. APS 23, 344 (1978).
2. A. Y. Wong, P. Leung and D. L. Eggleston, Phys. Rev. Lett. 39, 1407 (1977).

*Supported by AFOSR contract F-49620-76-C-0011.

EXPERIMENTAL APPARATUS

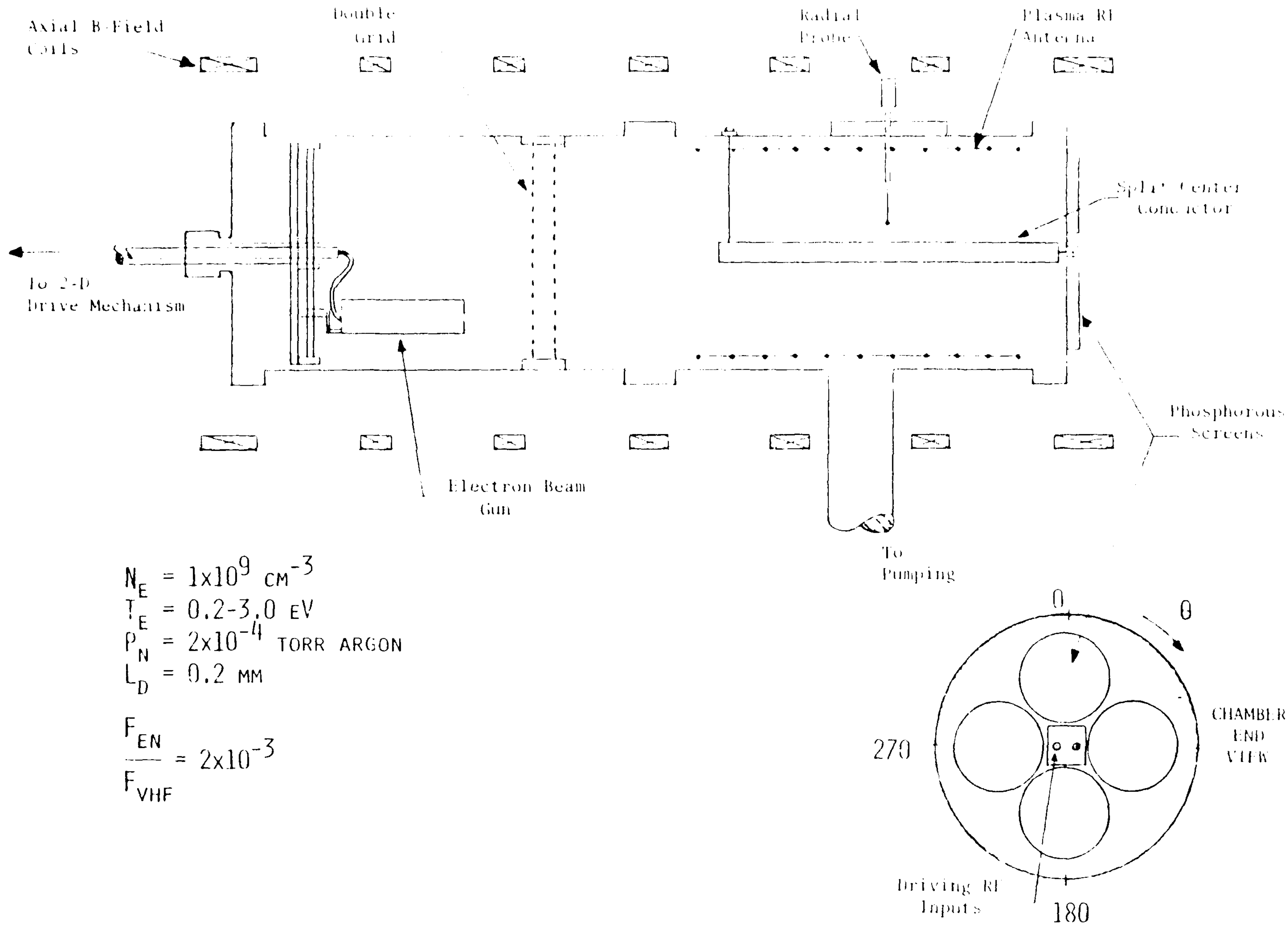

$N_E = 1\times10^9\ \mathrm{CM}^{-3}$
$T_E = 0.2\text{-}3.0\ \mathrm{EV}$
$P_N = 2\times10^{-4}$ TORR ARGON
$L_D = 0.2\ \mathrm{MM}$

$$\frac{F_{EN}}{F_{VHF}} = 2\times10^{-3}$$

Figure 1

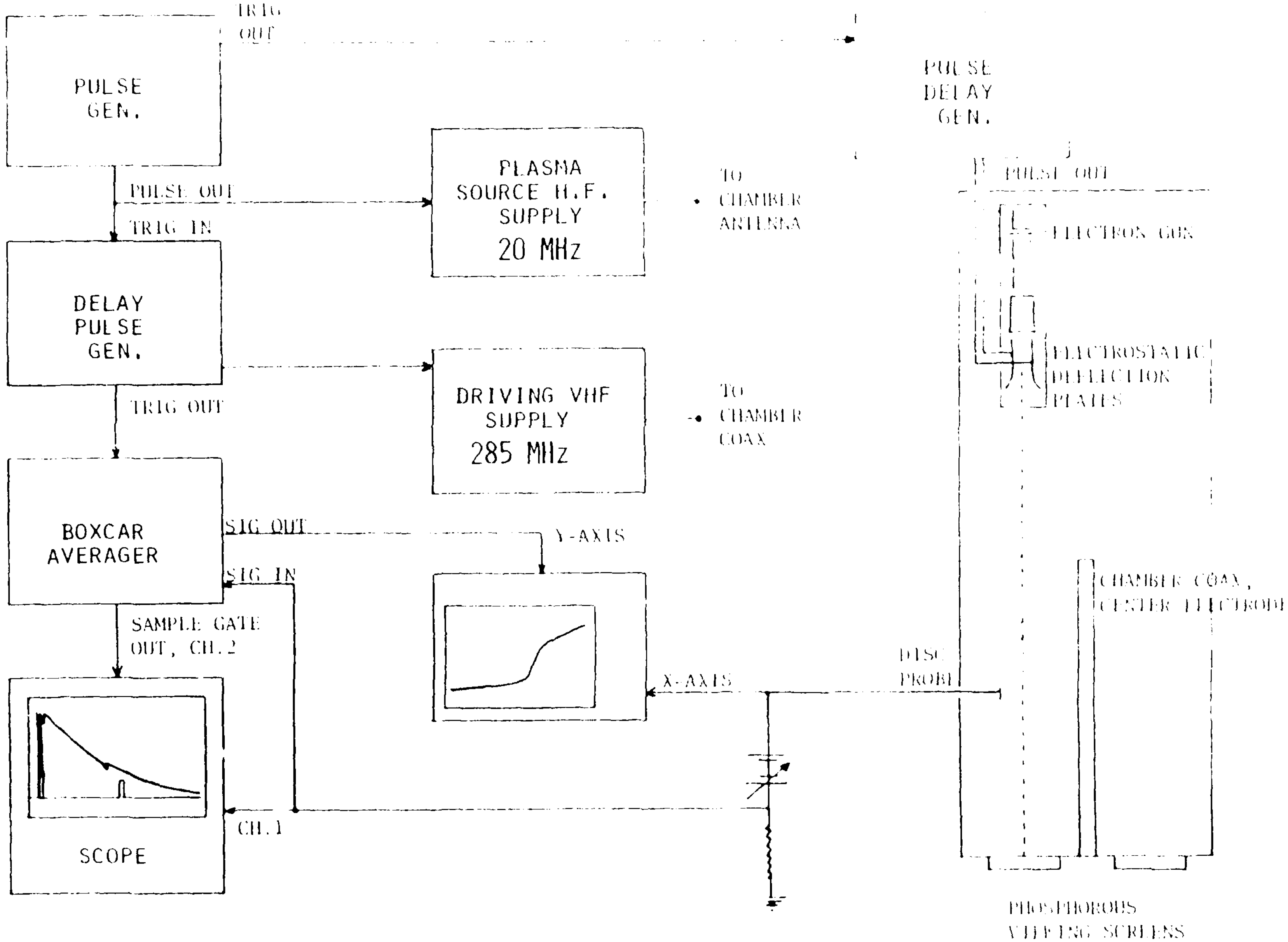

PULSE GEN.
TRIG OUT
PULSE OUT
TRIG IN
DELAY PULSE GEN.
TRIG OUT
BOXCAR AVERAGER
SIG OUT
SIG IN
SAMPLE GATE OUT, CH.2
SCOPE
CH.1
PLASMA SOURCE H.F. SUPPLY 20 MHz
TO CHAMBER ANTENNA
DRIVING VHF SUPPLY 285 MHz
TO CHAMBER COAX
Y-AXIS
X-AXIS
PULSE DELAY GEN.
PULSE OUT
ELECTRON GUN
ELECTROSTATIC DEFLECTION PLATES
CHAMBER COAX, CENTER ELECTRODE
DISC PROBE
PHOSPHOROUS VIEWING SCREENS

Figure 2

Figure 3

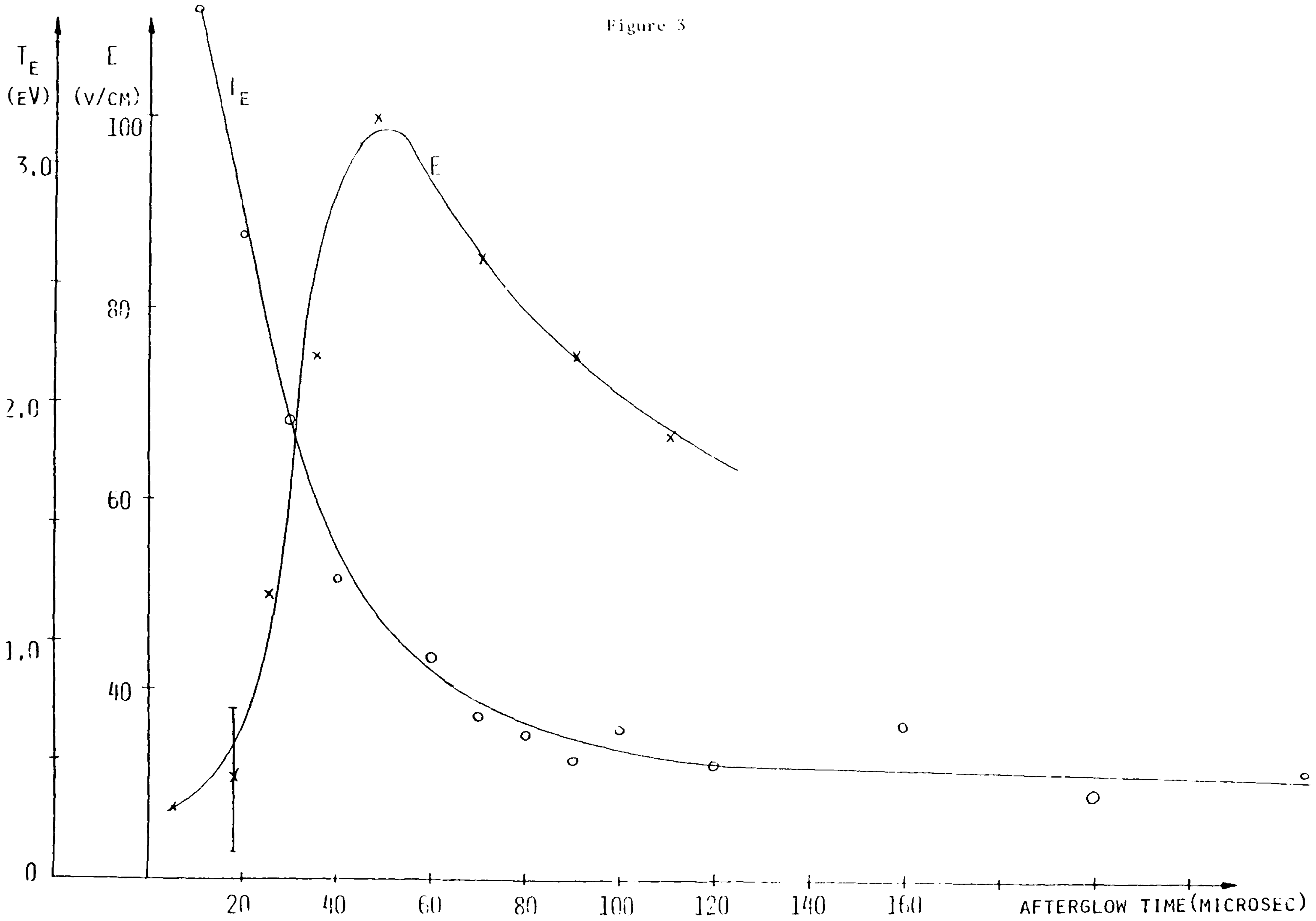

T_E (eV)
E (V/CM)
100
80
60
40
3.0
2.0
1.0
0
T_E
E
20
40
60
80
100
120
140
160
AFTERGLOW TIME (MICROSEC)

Figure 4

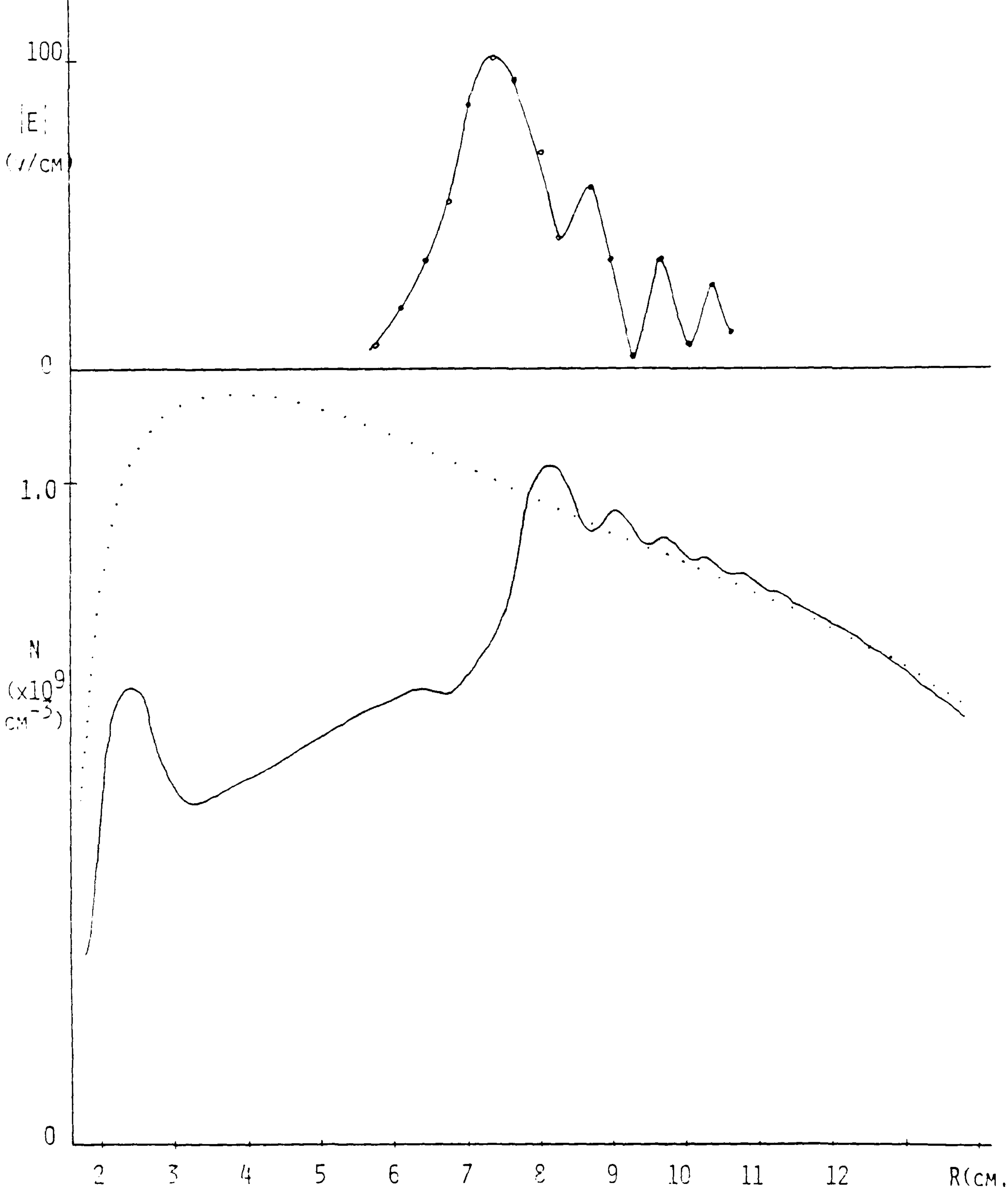

Figure 5

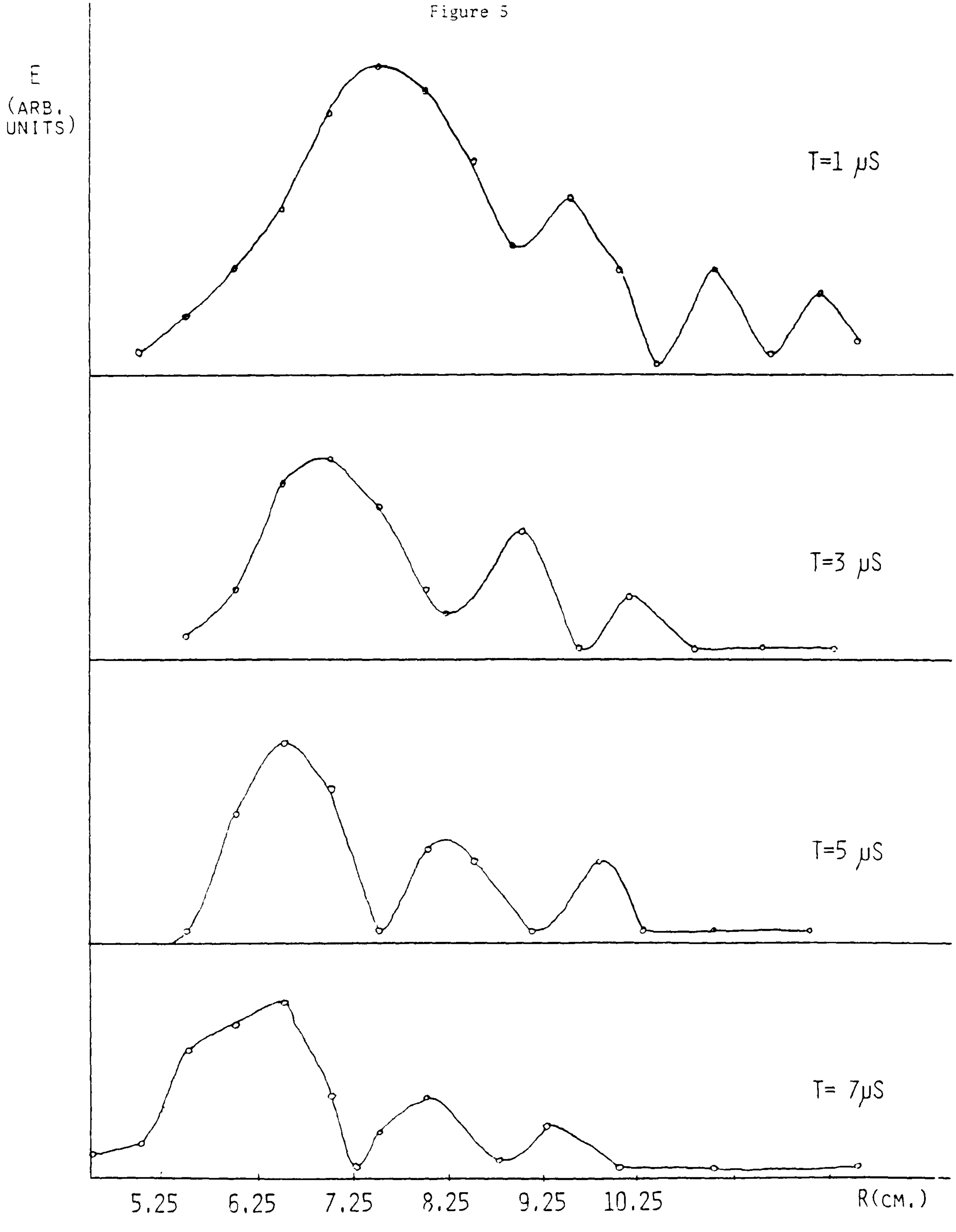

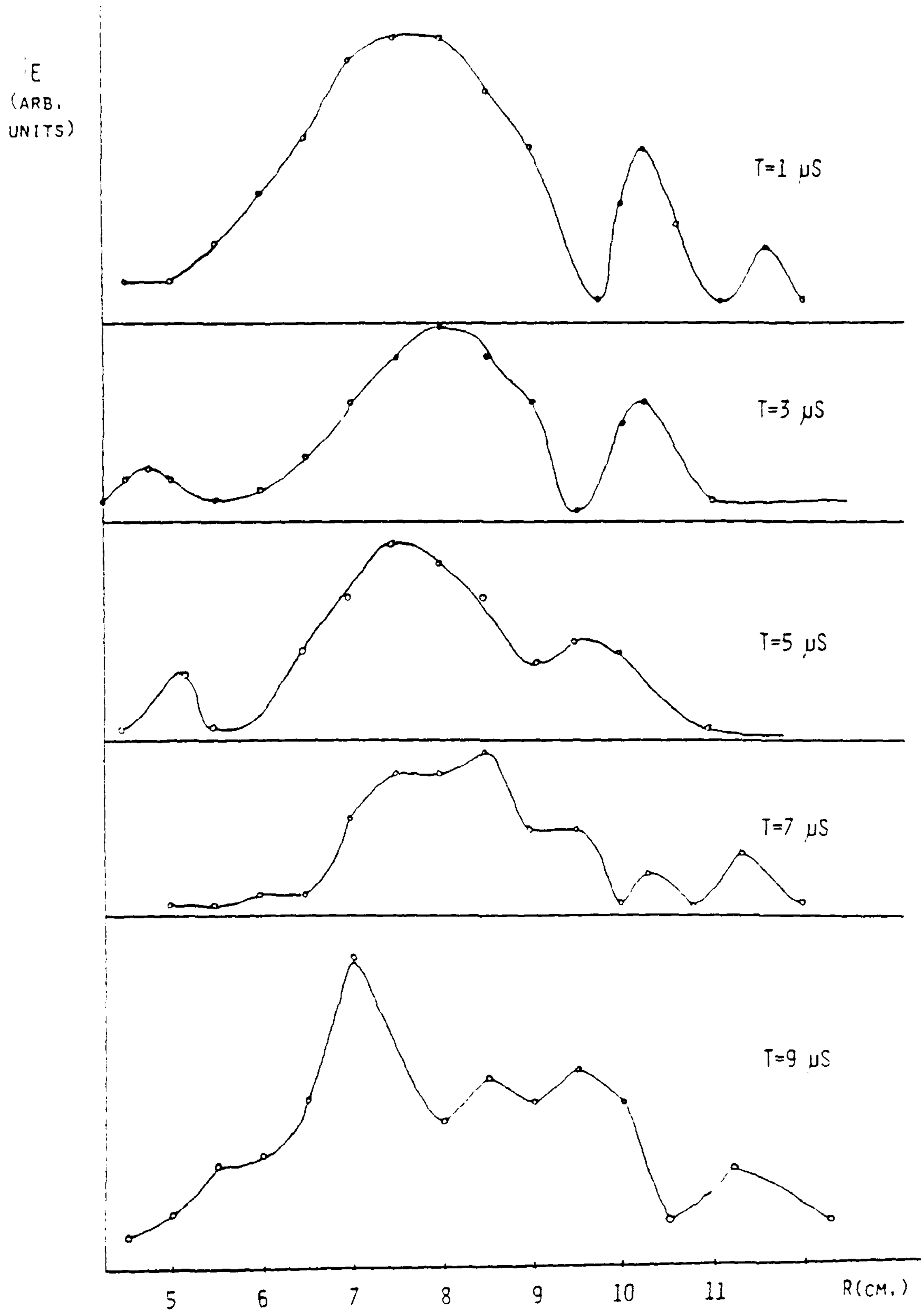

Figure 6

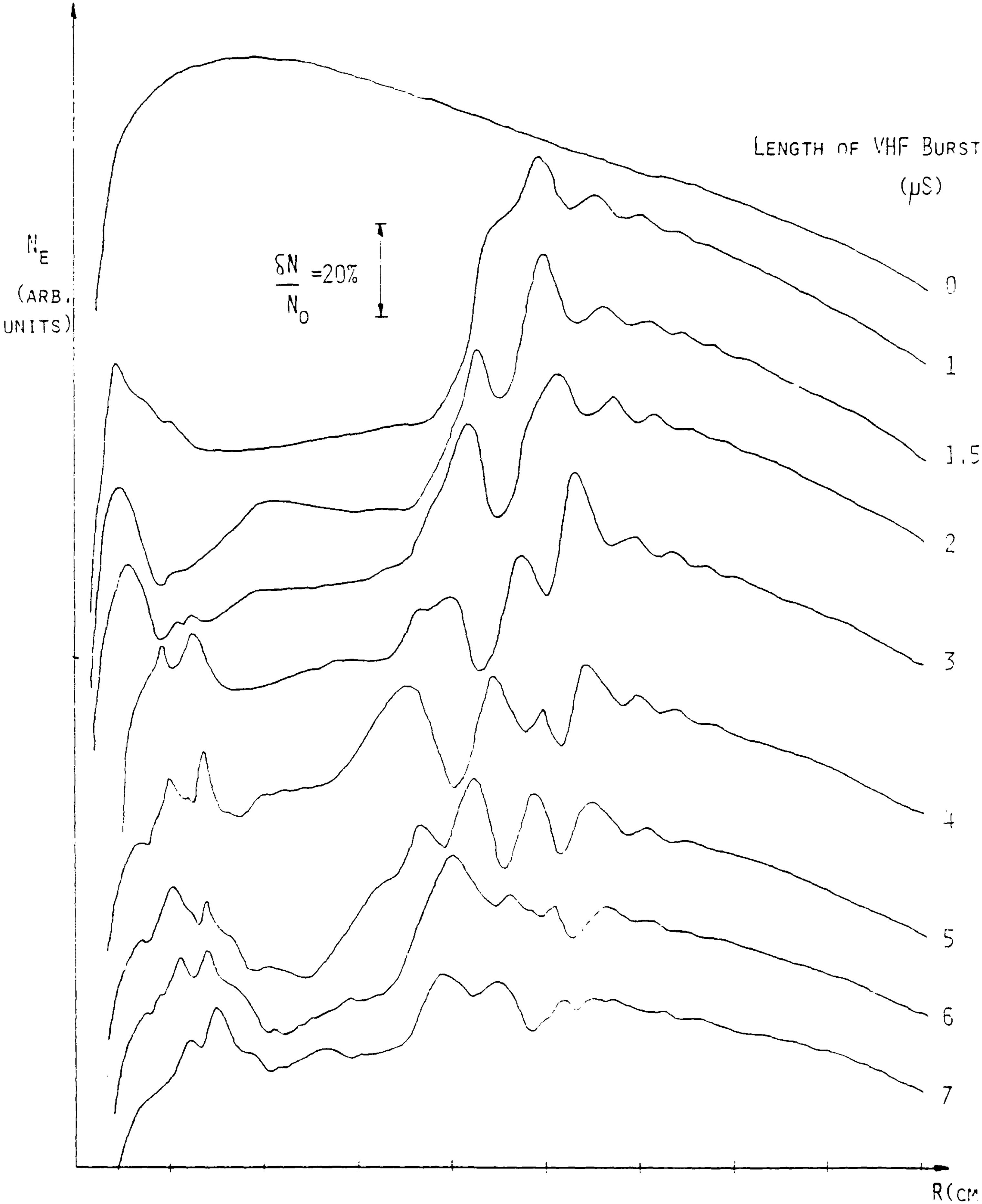
LENGTH OF VHF BURST
(μS)
N_E
(ARB. UNITS)
$\frac{\delta N}{N_0}$ =20%
0
1
1.5
2
3
4
5
6
7
R(CM

Figure 7

Figure 8

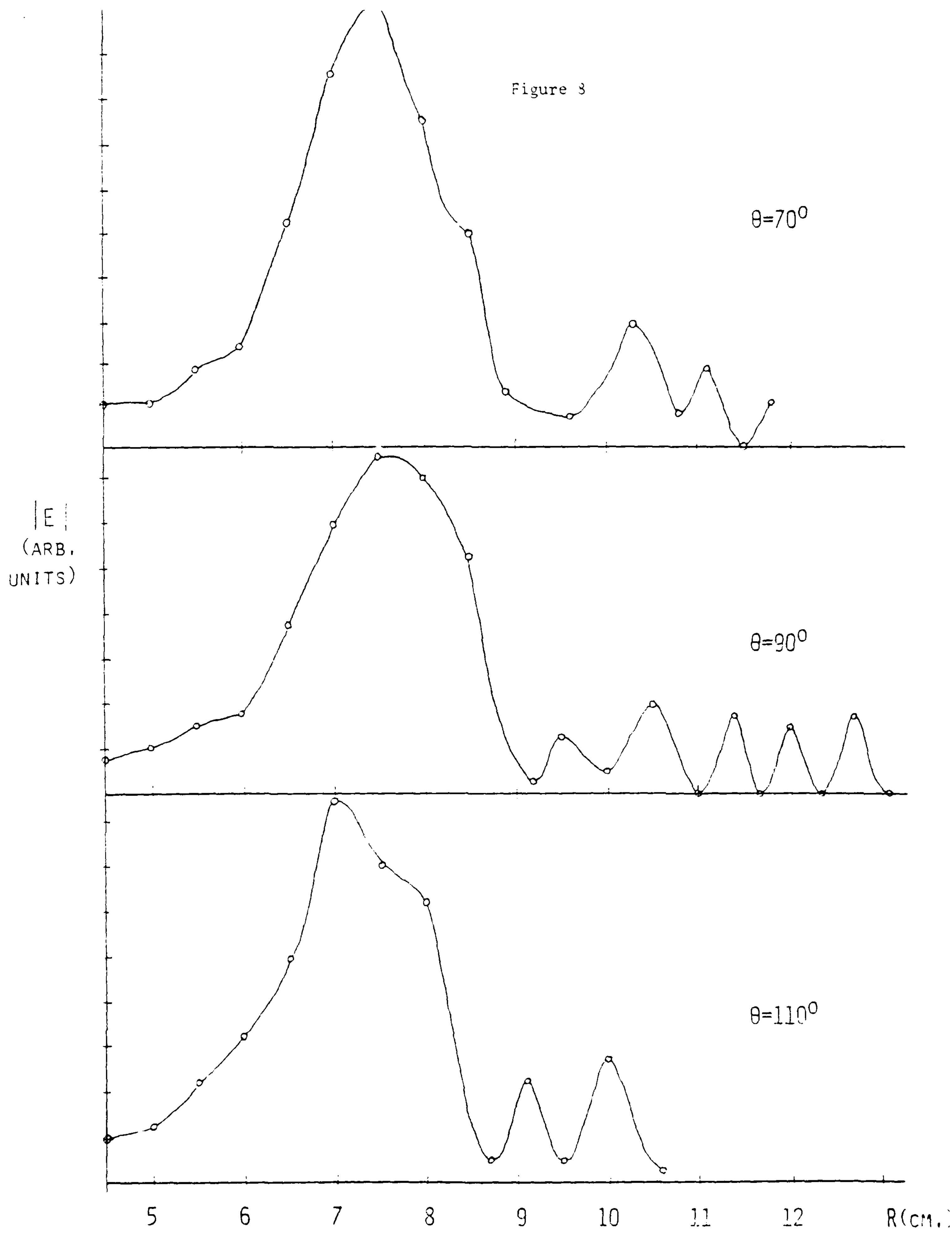

Figure 9